Model Calculations of the Structure of Ni–Nb Metallic Glasses

P. Lamparter

Max-Planck-Institut für Metallforschung, Institut für Werkstoffwissenschaft, Seestrasse 92,
D-70174 Stuttgart

Z. Naturforsch. **50a,** 329–336 (1995); received January 9, 1995

The partial pair correlation functions of amorphous Ni_xNb_{100-x} alloys ($x=40$, 50, 56, and 63) were simulated by computer modelling. A Cluster Relaxation procedure yielded reasonable agreement with the experimental functions when non-additive pair potentials with preference for Ni–Nb atomic pairs were applied. With the use of the Reverse Monte Carlo method perfect agreement could be achieved. The impact of the chemical effect on the short range order is discussed by comparison with a statistical reference cluster. The analysis of the model clusters showed that the chemical short range order effect in amorphous Ni–Nb alloys, increasing with the Ni concentration, does not involve specific stereochemical atomic arrangements. There is no correspondence to the short range order in crystalline Ni_3Nb. The structure of Ni–Nb metallic glasses can be described as a polytetrahedral packing with preferred hetero-coordination.

1. Introduction

The concentration dependence of the atomic structure of melt-spun Ni_xNb_{100-x} metallic glasses ($x=40$, 50, 56, and 63) has been investigated in [1]. The partial pair correlation functions were established by neutron diffraction using isotopic substitution. The experimental study revealed that amorphous Ni–Nb alloys are characterized by a chemical short range order (CSRO) effect which is stronger at higher Ni concentration, as well as by a distinct size effect (SE).

Concerning the nature of the CSRO in metallic glasses two different points of view may be found in the literature:

i) Regions with a higher degree of order, so-called associates, are embedded in a matrix, where the distribution of the constituents is statistical. Within this view the system is inhomogeneous, and the measured structural parameters represent average values of the parameters in the regions and in the matrix. The degree of the CSRO, e.g. given by a short range order parameter, is determined by the number of ordered regions.
ii) The system is essentially homogeneous. The chemical interaction between unlike atoms causes a certain preference for hetero-coordination. The degree of the CSRO is determined by the statistical number of unlike atomic pairs compared to the number of like atomic pairs.

A further related question concerns structural units in an amorphous system, i.e. the question whether or not the CSRO is associated with specific coordination polyhedra, and if so, whether or not these correspond to the short range order in related crystalline phases.

In [1] it has been reported that the partial coordination numbers around Ni in the four investigated Ni–Nb glasses extrapolate well to the corresponding numbers in crystalline Ni_3Nb, which gives rise to the question, how the Nb and Ni atoms are arranged spatially around the Ni atoms.

For a discussion of these questions we need information about the three-dimensional arrangement of the atoms and about the site-to-site variation of local structural properties. In the present work three-dimensional atomic clusters were constructed by using a Cluster Relaxation (CR) program as well as the Reverse Monte Carlo (RMC) method. As guideline for the computer simulations the experimental pair correlation functions $G_{ij}(R)$ from [1] were employed, which are defined as

$$G_{ij}(R) = 4\pi R\,[\varrho_{ij}(R)/c_j - \varrho_0]\,, \tag{1}$$

where $\varrho_{ij}(R)$ is the number of j-type atoms per volume at the distance R from an i-type atom at the origin, and ϱ_0 is the mean number density.

For a detailed presentation of the definitions and equations for the structural description of amorphous alloys see e.g. the review by Lamparter and Steeb [2]. An RMC simulation on amorphous $Ni_{62}Nb_{38}$ has been carried out by Pusztai and Sváb [3].

Reprint requests to Dr. P. Lamparter.

0932-0784 / 95 / 0400-0329 $ 06.00 © – Verlag der Zeitschrift für Naturforschung, D-72027 Tübingen

Alloy	R_0/Å			V_0/rel. un.			R_m/rel. un.		
	Ni–Ni	Ni–Nb	Nb–Nb	Ni–Ni	Ni–Nb	Nb–Nb	Ni–Ni	Ni–Nb	Nb–Nb
$Ni_{40}Nb_{60}$	2.70	2.90	3.25	0.8	1.0	1.0	1.40	1.30	1.00
$Ni_{50}Nb_{50}$	2.71	2.86	3.27	0.8	1.3	1.0	1.40	1.30	1.00
$Ni_{56}Nb_{44}$	2.68	2.86	3.27	0.8	1.5	1.0	1.40	1.30	1.00
$Ni_{63}Nb_{37}$	2.73	2.85	3.34	0.8	1.7	1.0	1.40	1.30	1.00
$Ni_{63}Nb_{37}$ [a]	2.80	3.07	3.34	1.0	1.0	1.0	1.30	1.30	1.30

Table 1. Parameters of the pair potentials for the CR models. R_0, V_0 = position, depth of the minimum, R_m = range of interaction, normalized to R_0.

[a] Statistical reference system.

2. Model calculations

2.1. Cluster Relaxation

The partial pair correlation functions $G_{ij}(R)$ were simulated using a static version of a Molecular Dynamics algorithm given by Brandt [4, 5]. An atomic cluster of 1500 atoms was relaxed under the influence of parabolic pair potentials whose specific shape is determined by 4 adjustable parameters, describing the position R_0 and depth V_0 of the minimum, the range R_m of interaction, and the exponent $k=n+2$ of the repulsive term:

$$V(R) = a r^2 [r^n - b] V_0 , \qquad (2)$$

where

$$r = (R_m - R)/(R_m - R_0) ,$$
$$a, b = 1/2, 3 \quad \text{for} \quad n=4 ,$$
$$a, b = 1/3, 4 \quad \text{for} \quad n=6 .$$

The fitting parameters were varied until optimum agreement between the model and the experimental $G_{ij}(R)$ was observed. The values of the fitting parameters are listed in Table 1. The choice of a stronger repulsion for Ni–Ni pairs, $k=8$, than for Ni–Nb and Nb–Nb pairs, $k=6$, yielded the best results. The $G_{ij}(R)$ functions of the model clusters in Fig. 1 (dashed) show reasonable agreement with the experimental functions (dotted).

Although a determination of realistic pair potentials of Ni–Nb glasses is out of the scope of the present study (this has been done by Hausleitner and Hafner [6, 7]), some qualitative conclusions may be drawn:

i) The potentials are non-additive. There is a chemical contraction of the Ni–Nb distance with respect to the average of the Ni–Ni and the Ni–Nb distances.

ii) With increasing Ni content the Ni–Nb interaction becomes stronger, which is in accordance with the experimentally observed increase of the CSRO.

iii) In the $Ni_{40}Nb_{60}$ alloy the interaction between Ni and Nb is not stronger than the interaction in Nb–Nb pairs and only slightly stronger than in Ni–Ni pairs. With the choice of a stronger Ni–Nb interaction parameter it was not possible to obtain a good fit of the amplitude of the first peak in the Ni–Ni correlation function. It became too high.

2.2. Reverse Monte Carlo

The RMC calculations were performed by using a computer algorithm from McGreevy and Pusztai [8]. As starting configuration for each alloy the cluster from the CR simulation was taken. The RMC refinement was performed within about 2000 accepted displacements per atom. The distance of closest approach in i–j pairs was taken from the onset of the first peak of the experimental $\varrho_{ij}(R)$ curve. For the number density ϱ_0 of the 4 Ni_xNb_{100-x} alloys the values 0.066, 0.070, 0.071, and 0.073 Å^{-3} (with increasing x) were used in the RMC runs. As the CR clusters already represent a good description of the experimental data, the RMC refinement reached quite quickly the final configuration, i.e. the state of equilibrium where no further improvement was observed. The agreement between the $G_{ij}(R)$ functions of the RMC clusters (solid lines) and the experimental functions (dotted) in Fig. 1 is excellent. From this we state that the three partial pair correlation functions, as established by the isotopic substitution method, represent a mutual consistent set in the sense that a corresponding three-dimensional arrangement of Ni and Nb atoms is possible.

It should be noted that the experimental density-concentration correlation functions [1] according to the Bhatia and Thornton notation [9] are of course described with the same quality by the RMC models.

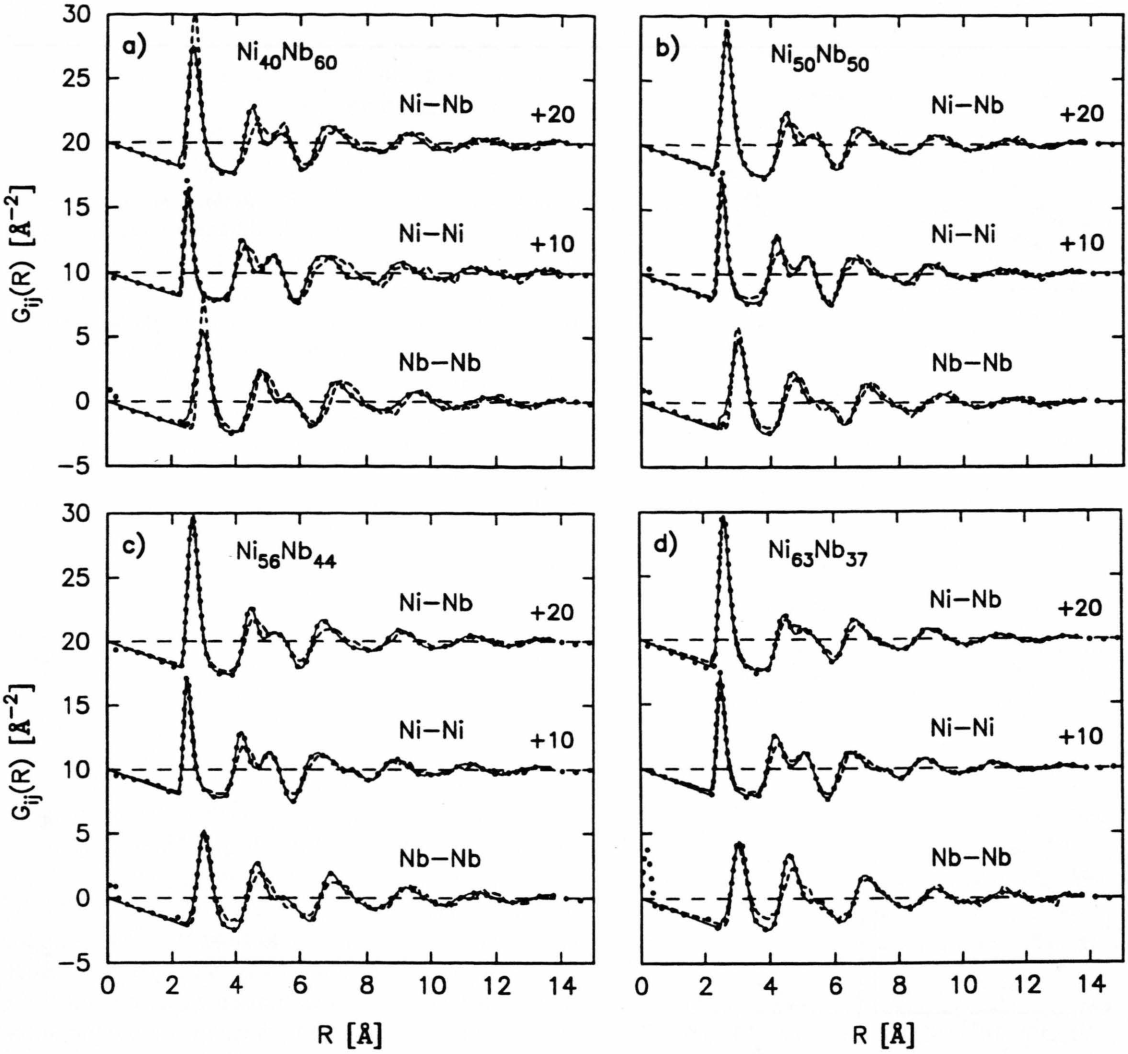

Fig. 1. Amorphous Ni–Nb alloys: partial pair correlation functions. ··· experimental [1], --- Cluster Relaxation (CR) model, — Reverse Monte Carlo (RMC) model.

3. Analysis of the model clusters

3.1. Coordination numbers

The partial coordination numbers Z_{ij} were determined from the coordinates of the RMC clusters taking as outer limit of the i–j coordination sphere the minimum between the first and the second peak in the corresponding radial distribution function $\mathrm{RDF}_{ij}(R) = 4\pi R^2 \varrho_{ij}(R)$. The histograms in Fig. 2 show that the distributions of coordination numbers in the Ni–Nb glasses are rather broad, extending over a spread of variation of 5 to 6 in the total Z_i and of 6 to 7 in the partial Z_{ij}. For example, the number of Ni–Ni neighbours in $Ni_{63}Nb_{37}$ (Fig. 2a) lies in the range $3 \leq Z_{\mathrm{NiNi}} \leq 9$. From this observation alone it is clear that amorphous Ni–Nb alloys, as metallic glasses in general (see e.g. [10]), are not built as assemblies of a certain type of structural unit, which is in contrast to the group of covalent glasses.

In approaches to keep the concept of structural units in metallic glasses, sometimes the co-existence of several different specific units has been suggested, and to a certain coordination number a certain type of

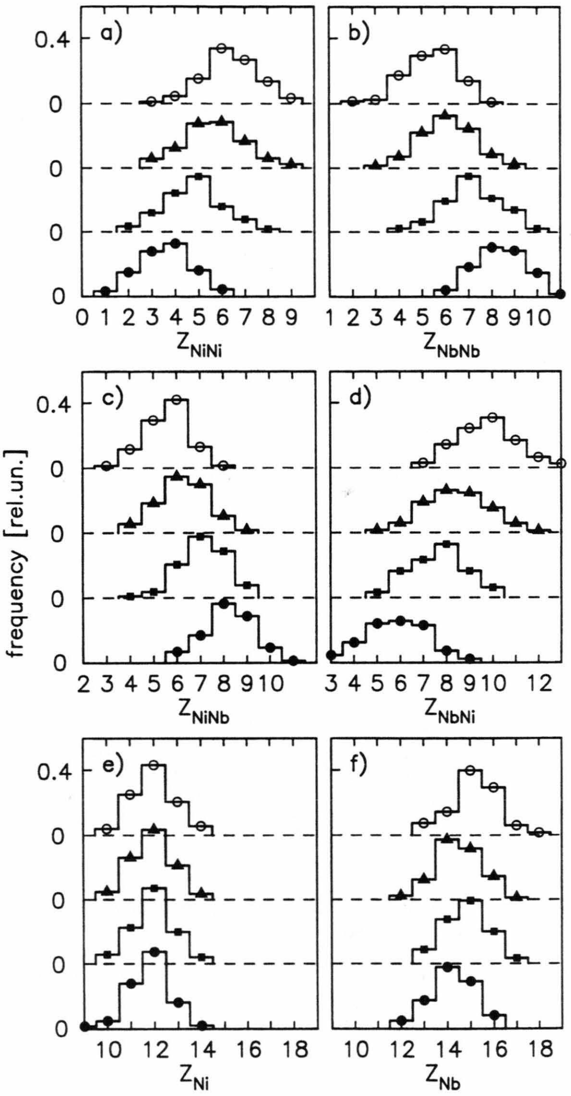

Fig. 2. Amorphous Ni–Nb alloys: histograms of partial coordination numbers Z_{ij} (j around i) and total coordination number $Z_i = Z_{ij} + Z_{ii}$, from RMC model. ● 40% Ni, ■ 50% Ni, ▲ 56% Ni, ○ 63% Ni.

coordination polyhedron was attributed. However, we note that a detailed analysis of the clusters in the present work did not give any evidence that a certain coordination number Z is associated at the same time with a certain type of three-dimensional arrangement of the Z neighbours. Furthermore, the experimentalists know well that the distributions depend to a certain extend on the definition of the nearest neighbour coordination shell, i.e. on the method to separate it from the partly overlapping second shell. For example, a slight enlargement of the upper integration limit causes an increase of the coordination number from Z to $Z+1$ for a number of atoms, of course without affecting the given arrangement of the Z neighbours, which means a shift of the distribution towards higher Z. Altogether, we state that the distributions of coordination numbers in Ni–Nb glasses are continuous, and that a classification into different specific coordination polyhedra is not suggested.

Figure 3a shows the concentration dependence of the widths of the histograms of the partial coordination numbers in Figure 2. There is an overall trend that the distributions become slightly sharper with increasing Ni concentration, i.e. with increasing CSRO. However, the widths are sharper at 50% Ni than at the neighbouring concentrations 40% Ni and 56% Ni. Such a dip in the concentration dependence has already been observed with the chemical contraction of the Ni–Nb distance and, less distinctly, with the short range order parameter, as shown in Figure 3b. The question whether this feature is real or due to some uncertainty in the experimental data has not been discussed in [1]. As the dip in Fig. 3a is connected with a property resulting from RMC models (though RMC is based on the experimental data), and as it can be hardly conceived that a certain experimental error may affect in the same way such different physical parameters as shown in Figs. 3a and 3b, it is suggested that it is real. That means, it is suggested that the increase of the CSRO going from 40% Ni to 63% Ni is not uniform, but a region around 50% Ni is passed, where the ordering tends to be stronger. In further investigations of this question an experimental technique should be employed which allows the measurement of a continuous series of Ni_xNb_{100-x} glasses at more than 4 compositions, and which is sensitive to one of the ordering effects, e.g. to the contraction of the Ni–Nb distance.

The widths of the distributions in Fig. 3a around a central Ni atom are smaller than those around a central Nb atom. This points to a higher degree of order around the Ni atoms. An asymmetric behaviour of the short range order with respect to the two constituents in Ni–Nb glasses has been already reported in [1].

3.2. Bond angles

In the following, the atomic order around the Ni atoms is considered. The bond angle distributions of

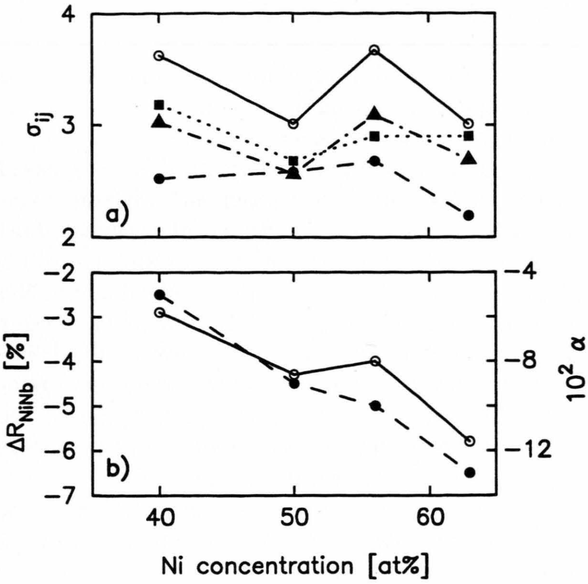

Fig. 3. Amorphous Ni–Nb alloys: a) width (FWHM) of the distributions of the partial coordination numbers, from RMC; ● Ni–Nb, ▲ Ni–Ni, ■ Nb–Nb, ○ Nb–Ni. b) ○ chemical contraction of the Ni–Nb distance compared to the mean value of the Ni–Ni and Ni–Nb distances, ● short range order parameter, from [1].

the RMC clusters in triplets with a Ni atom at the vertex are presented in Figure 4. The distributions display two peaks: a first one between 60° and 70° and a second one between 110° and 120° (between 170° and 180° a bump is indicated). Such a two-peak structure in the bond angle distributions is generally observed with metallic glasses and thus is not significant for any specific ordering effects apart from a tetrahedral packing of the atoms.

The 60° angle appears in a tetrahedron of atoms with equal size. The larger bond angle in Nb–Ni–Nb triplets (Fig. 4c) than in Ni–Ni–Ni triplets (Fig. 4a) can be explained geometrically by the larger size of the Nb atoms compared with that of the Ni atoms. The concentration dependence of this Nb–Ni–Nb angle displays a shift of the peak towards larger angles with increasing Ni content, which is explained by the increasing Nb–Nb distance (from 2.98 Å to 3.06 Å) and the decreasing Ni–Nb distance (from 2.66 Å to 2.62 Å), as observed experimentally in [1]. The arrows in Fig. 4 mark the bond angles calculated for nearest neighbour triplets, where the experimental atomic distances were used.

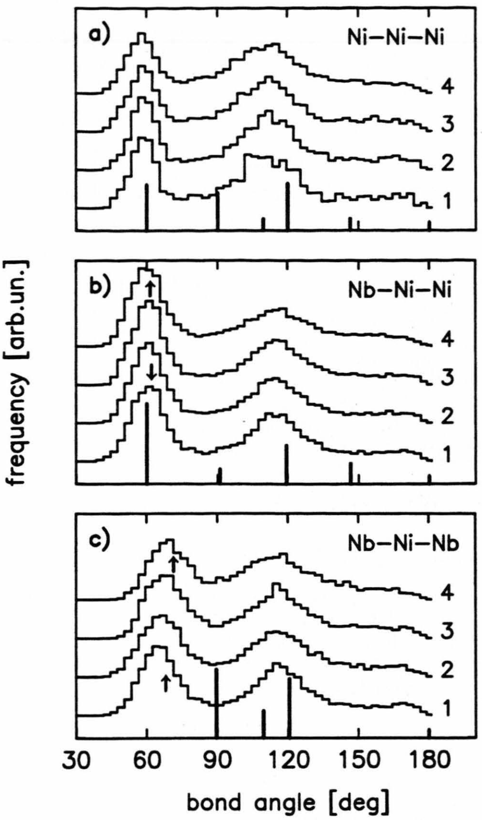

Fig. 4. Amorphous Ni–Nb alloys: histograms of bond angles from RMC model. 1: 40%, 2: 50%, 3: 56%, 4: 63% Ni; the bars are for crystalline Ni_3Nb; the arrows mark the angles in atomic triples with distances corresponding to the peak positions of the experimental $G_{ij}(R)$ in Fig. 1 for 40% and 63% Ni.

Figure 5a shows the average distances in Nb–Ni–Nb triplets for the RMC cluster of $Ni_{63}Nb_{37}$ in dependence of the Nb–Ni–Nb bond angle. The run of these curves in the bond angle range of the first peaks in Fig. 4c shows again (now within one single atomic configuration) the correlation between the increasing Nb–Ni–Nb bond angle and the decreasing Ni–Nb and increasing Nb–Nb distances.

As for the second peak in the bond angle distributions between 110° and 120°, it should be mentioned that by placing a further atom on a face of a tetrahedron an angle of 109.5° occurs.

With increasing Ni concentration the bond angle distributions tend to become more smeared out, which is interesting to note in the light of the increasing CSRO. Specific structural ordering phenomena,

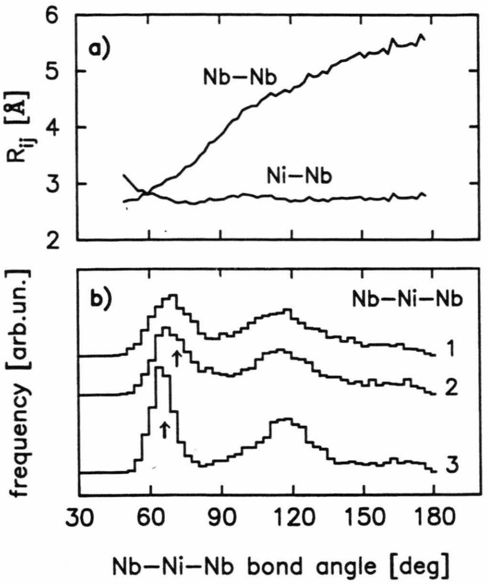

Fig. 5. Amorphous $Ni_{63}Nb_{37}$: a) mean distances in Nb–Ni–Nb triplets in dependence of the Nb–Ni–Nb angle, from RMC model. b) histograms of Nb–Ni–Nb bond angles. 1: RMC model, as in Fig. 4c, 2: CR model with CSRO, 3: CR model, statistical reference system.

deviating from polytetrahedral packing, are not observed with any of the bond angle distributions in Figure 4. In particular, with increasing Ni content there are no peculiarities observed, such as the appearance of additional bond angles. From this we have to conclude that the CSRO in Ni–Nb glasses, increasing with the Ni content, does not promote specific stereochemical atomic arrangements. The viewpoint of so-called associates is not supported.

As a representative example for a comparison between the RMC model and the CR model, the Nb–Ni–Nb bond angle distributions in amorphous $Ni_{63}Nb_{37}$ are shown in Fig. 5b (curves 1 and 2). The distributions are essentially the same, and we state that, in the light of bond angles, the CR method, though employing potentials, does not create a higher degree of order than the RMC method. Because of this observation, and because RMC generally creates the most disordered configuration consistent with the experimental pair correlation functions, it seems to be probable, that also the structure of the real Ni–Nb glasses is most disordered within the constraints of the size effect and the specific degree of hetero-coordination.

4. Statistical reference system

For a characterization of the type and of the degree of ordering phenomena in an amorphous alloy comparison with two reference systems is often made: a statistical reference system where the different types of atoms are distributed at random, and a reference system with highest possible degree of chemical short range order. This is also useful for examining, which structural features are due to the chemical interaction between the constituents (CSRO) and which are due to the different atomic sizes (SE). However, the definition of a statistical reference system is not unequivocal, which complicates the characterization of the CSRO in a quantitative way, e.g. by using the concept of short range order parameters (cf. [10]).

One possible way to define a statistical reference system is to construct a cluster, by Cluster Relaxation or by Molecular Dynamic, which contains the size effect by proper choice of the atomic diameters, but where the interaction parameters do not involve a preference for specific atomic pairs. Figure 6 shows for the $Ni_{63}Nb_{37}$ alloy the partial $G_{ij}(R)$ of a statistical CR model (solid lines). The Ni–Ni and Nb–Nb distances were chosen to match the experimental distances, i.e. to include the SE, and the Ni–Nb distance as the arithmetic mean (Table 1). For comparison also the $G_{ij}(R)$ of the CR model from Fig. 1d, which includes the CSRO, are plotted in Fig. 6 (dashed). The impacts of the chemical Ni–Nb interaction on the

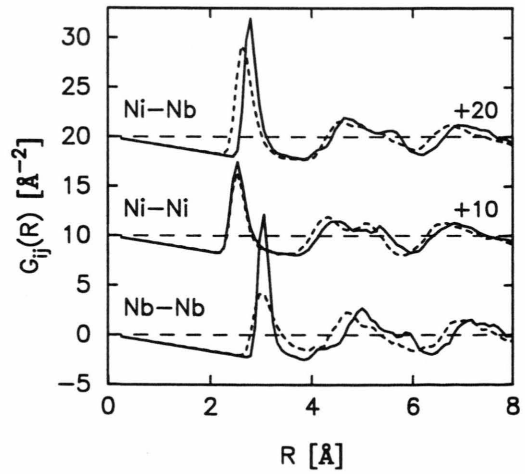

Fig. 6. Amorphous $Ni_{63}Nb_{37}$: partial pair correlation functions from CR models. — statistical reference system; --- with CSRO, same curves as in Figure 1d.

structure are:

i) A contraction of the Ni–Nb distance; but interestingly no increase of the Ni–Nb coordination number.
ii) Almost no change of the Ni–Ni correlation.
iii) The strongest impact is observed with the Nb–Nb correlation, and not with Ni–Nb as one might have expected. The Nb–Nb nearest neighbour correlation becomes much less defined, and the Nb–Nb coordination number is smaller than in the statistical system by about one Nb atom. Apparently, the preference for hetero-coordination, with respect to a statistical distribution, is associated with a decrease of Nb–Nb pairs rather than with an increase of Ni–Nb pairs.

The Nb–Ni–Nb bond angle distribution of the statistical system is included in Fig. 5b (curve 3). Comparison with curves 1 and 2 shows that the introduction of CSRO into the system causes a shift of the first peak towards larger angles, due to the contraction of the Ni–Nb distance. It causes also a broadening of the peak, which is in line with the observation in Fig. 6 that the Nb–Nb distance distribution is wider in the system with CSRO than in the statistical system. The broadening is also in line with the increasing smearing of the bond angle distributions in the RMC models, due to the increasing CSRO (Figure 4).

5. Comparison with crystalline Ni_3Nb

The increase of the CSRO in Ni–Nb glasses at higher Ni concentration, as well as the fact that the partial coordination numbers around the Ni atoms in the glasses extrapolate well to the corresponding numbers in the crystalline phase Ni_3Nb [1] give rise to the question whether the three-dimensional arrangement of the Ni and the Nb atoms around Ni is similar in both states of matter. The structure of orthorhombic Ni_3Nb is of the Cu_3Ti type with two lattice sites (b and f) of the Ni atoms [11]. Figure 7 shows the coordination sphere of a Ni(f) atom, consisting of 4 Nb and 8 Ni neighbours. The coordination sphere of the Ni(b) atoms has the same characteristic features, as far as bond angles are concerned. The most distinct structural feature in Ni_3Nb, in contrast to a tetrahedral packing, is the arrangement of the atoms on square faces, yielding a strong contribution at the angle of 90° in the bond angle distributions in Figure 4. Such a contribution is not found with the amorphous Ni–Nb alloys, and there is no trend towards it with increasing Ni content. Moreover, the missing 60° angle in the Nb–Ni–Nb distribution of crystalline Ni_3Nb is in distinct contrast to the metallic glasses.

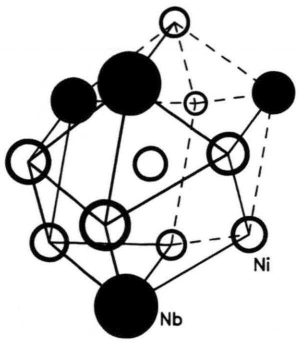

Fig. 7. Crystalline Ni_3Nb: coordination sphere of a Ni(f) atom.

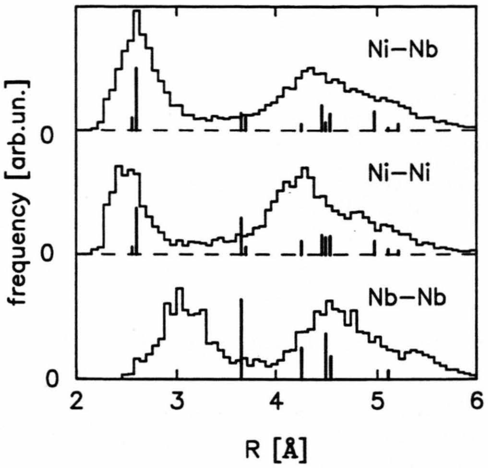

Fig. 8. Amorphous $Ni_{63}Nb_{37}$ and crystalline Ni_3Nb: histograms of distances between atoms in the first coordination shell of a Ni atom; for $Ni_{63}Nb_{37}$ from RMC.

A further characterization of the arrangement of the atoms around a central Ni atom is given in Figure 8. It shows the distances between the atoms which belong to the same coordination shell around a Ni atom for the RMC cluster of the $Ni_{63}Nb_{37}$ glass and for crystalline Ni_3Nb. (Note, that the constraint of the same coordination shell assigns the meaning of a triplet correlation to the functions in Figure 8.) Apart from some accordance of the nearest Ni–Ni and Ni–

Nb distances, which is trivial, no similarities are observed.

Altogether we state that the triplet correlations do not suggest any correspondence in the stereochemical ordering in amorphous Ni–Nb alloys and in the crystalline phase Ni_3Nb.

6. Conclusions

The partial pair correlation functions of amorphous Ni_xNb_{100-x} alloys ($x = 40$, 50, 56, and 63) can be simulated with good agreement with the experimental data by Cluster Relaxation, using appropriate pair potentials, and with perfect agreement by Reverse Monte Carlo models. The chemical interaction between the Ni atoms and the Nb atoms causes a slight preference for hetero-coordination in the glasses, which increases with the Ni concentration. The chemical short range order does not involve specific stereochemical coordination polyhedra deviating from a polytetrahedral packing. The three-dimensional ordering of the atoms in the amorphous alloys shows no correspondence to the structure of crystalline Ni_3Nb.

Acknowledgement

Thanks are due to E. H. Brandt and to R. L. McGreevy for supplying the modelling programs.

[1] P. Lamparter, M. Schaal, and S. Steeb, Proc. Conf. Neutron and X-ray Scattering: Complementary Techniques, Kent, 1989, Inst. Phys. Conf. Ser. No. **101,** 51 (1990).
[2] P. Lamparter and S. Steeb, "Structure of Amorphous and Molten Alloys" in: Material Science and Technology, Vol. 1, VCH, Weinheim 1993, pp 217–288.
[3] L. Pusztai and E. Sváb, J. Non-Cryst. Solids **156–158,** 973 (1993).
[4] E. H. Brandt, J. Phys. F **14,** 2485 (1984).
[5] E. H. Brandt and H. Kronmüller, J. Phys. F **17,** 1291 (1987).
[6] Ch. Hausleitner and J. Hafner, Phys. Rev. B **45,** 115 (1992).
[7] Ch. Hausleitner and J. Hafner, Phys. Rev. B **45,** 128 (1992).
[8] R. L. McGreevy and L. Pusztai, Mol. Sim. **1,** 359 (1998).
[9] A. Bhatia and D. E. Thornton, Phys. Rev. B **2,** 3004 (1970).
[10] P. Lamparter and S. Steeb, Proc. 6-th Int. Conf. of the Structure of Non-Cryst. Mat., NCM6, Praha, Aug. 29–Sept. 2, 1994, J. Non-Cryst. Solids, submitted.
[11] W. B. Pearson, Lattice Spacings and Structures of Metals and Alloys, Vol. 2, Pergamon Press, London, New York 1967.